



# Moving Hydrogen through the UK Gas Distribution Network

Michael Sargent <sup>a,\*</sup>, Philip Sargent <sup>a</sup>

<sup>a</sup>Cambridge Energy UK, 27 Greville Road, Cambridge CB1 3QJ, UK

---

## Abstract

We state the appropriate thermodynamic and transport properties to use for the delivery of hydrogen through pre-existing natural gas distribution networks. We show that the flow is not as fully-turbulent as past work has assumed, that hydrogen makes the flow even less turbulent, and that the pipe friction calculation requires more careful treatment in this partially-turbulent regime.

We propose that the relevant final energy demand is the energy delivered as heated water. The different dew points of the flue gases from hydrogen versus natural gas combustion affect the boiler efficiency. This impacts the relative amount of hydrogen required to be delivered.

We find that to deliver the same amount of useful energy as hot water, hydrogen requires a gas velocity of  $3.076\times$  and a pressure gradient that is  $P \text{ ratio}\times$  higher. The compression power increase required to deliver hydrogen through the low pressure network is  $E \text{ ratio}\times$  that for natural gas.

**Keywords:** Hydrogen, pipe-flow, friction factor, natural gas, condensing boiler, gas velocity.

---

## 1. Introduction

A possible future for the UK gas network is to reuse parts of it to distribute hydrogen instead of natural gas[1, 2]. In recent years it has become apparent that reusing parts of the low pressure distribution grid is a very different problem from re-using the the intermediate pressure distribution grid or the transmission grid[3, 4].

While a high pressure transmission system for hydrogen may be required in the UK[5], this would largely be new construction built in parallel with the existing natural gas National Transmission System. However parts of the intermediate and low pressure distribution system would be repurposed from natural gas to carry hydrogen.

These are the questions we want to answer:

1. Can the pipework carry enough hydrogen to match the amount of energy delivered to domestic housing?
2. What are the pressure and gas velocity differences?
3. How much extra energy would be required to deliver the hydrogen?

### 1.1. Bossel

An early attempt at these calculations was made by Bossel[6] but he considered pure methane, not natural gas,

through a transmission pipe with assumed fully-turbulent flow. In the distribution system non-linear friction effects become significant and the flow is not fully-turbulent. Models which have used Bossel's number are inaccurate for distribution and may not be quite right for transmission either, quite apart from considering the wrong gas.

## 2. Standard gas and reference conditions

Data on the exact composition of natural gas in the UK national transmission system is sparse, as the gas is a mixture of different gas fields that are processed together, and the composition changes over time and varies across the network. There are regulatory limits on certain properties of the gas, including the Wobbe number (see Appendix E.3, density, and calorific value under defined conditions.



Table 1: Composition of NG at Fordoun NTS on 20th Jan.2021.[7]



	[mol/mol]		[mol/mol]
CH4	89.5514 %	iC5	0.0344 %
C2H6	5.1196 %	neoC5	0.0020 %
C3H8	1.3549 %	C6	0.2377 %
nC4	0.2162 %	CO2	2.0743 %
iC4	0.1269 %	N2	0.9354 %
nC5	0.3472 %		

As a concrete example, this paper uses the composition of the gas taken directly from an 84 bar NTS transmission pipe at Fordoun (near Aberdeen) on 20 Jan.2021[7] as the composition of natural gas (NG).

This gas has 11 components: methane, ethane, propane, n-butane, iso-butane, n-pentane, iso-pentane, neo-pentane,

---

\*Corresponding author: Michael Sargent  
Email addresses: michael.sargent@cambridgeenergy.uk  
(Michael Sargent ) , philip.sargent@cambridgeenergy.uk  
(Philip Sargent )

URL: 0000-0001-9129-29907 (Michael Sargent ) ,  
0000-0002-0968-4467 (Philip Sargent )

hexane (including traces of higher hydrocarbons), carbon dioxide, and nitrogen. The Peng-Robinson equation of state can be used to calculate the average properties of this mixture[8], see Appendix F.1. The mixture has a molecular weight of 18.359 g/mol, a higher heating value of 940.813 kJ/mol and a density of 0.83556 kg/m<sup>3</sup> at 8°C.

The conditions of the gas in the distribution network that were used for these and all other material properties are representative of gas in the Service Line pipe entering a UK home during winter. The temperature of the gas in the distribution network is not significantly different from that of the surrounding ground, and the ground temperature at the depth of the distribution network will be about 8° during the winter months on average[9]. The average pressure in the distribution network is taken to be 40 mbar above one atmosphere (1.05325 bar)[2, 10].

### 3. Delivering combustion energy through a pipe

In comparing the delivery of natural gas and hydrogen through a pipe system, the metric by which they must be evaluated is the delivery of the same heat to the consumer.

#### 3.1. Molar Properties

When dealing with natural gas, quantities of the gas are often expressed either as mass, or volume at standard temperature and pressure. However as we are comparing different compressible gases (see Appendix B), both in the transport as well as the chemical reaction of combustion, we shall work in moles of gas. An ideal gas obeys the ideal gas law, equation (1).

$$P V_{ideal} = n R T \quad (1)$$

where  $n$  is the number of moles of gas,  $R$  is the gas constant (8.3145 J/mol·K),  $P$  is the absolute pressure and  $T$  is the absolute temperature.

We account for non-ideality of the gases by using the compressibility factor,  $Z$ , which is the ratio of the actual volume to that of an ideal gas under the same conditions:

$$Z = \frac{V_{real}}{V_{ideal}} \quad (2)$$

$Z$  is related to the external conditions via the molar volume, the volume of one mole of gas,  $V_m$ , which is linearly proportional to  $Z$  by the conditions of the gas:

$$V_m = \frac{V_{real}}{n} = \frac{Z R T}{P} \quad (3)$$

#### 3.2. Energy delivered

For the flow of a fuel through a pipe, such as the distribution system which supplies natural gas to domestic homes, the energy supply may be calculated by equation (4).

$$Q = A v \frac{[HHV]}{V_m} \eta = A v [HHV] \frac{P}{Z R T} \eta \quad (4)$$

The left side of this equation,  $Q$ , is the rate at which useful combustive energy is transferred along the pipe, in kJ/s.  $A$  is the cross section area of the supply pipe in m<sup>2</sup>.  $v$  is the linear velocity of the gas in m/s, which is the parameter that may be controlled to modify the rate of energy transfer to account for differences between the two gases.

The important gas properties are the molar volume,  $V_m$ , in m<sup>3</sup>/mol, and the Higher Heating Value, [HHV], also called the heat of combustion, in kJ/mol. Lastly,  $\eta$  is the efficiency of combustion reactions of the gases within domestic boiler systems.

To calculate the difference in gas velocity required for hydrogen compared to natural gas, equation (4) is calculated for each gas<sup>1</sup> for the same value of  $Q$ , and then the ratio of the two gives equation (5). We are considering the two gases in the same section of the distribution system, thus the pipe cross section area  $A$  and the temperature  $T$ , which should be equal to the ground temperature, are not included as they will be the same for both gases.

$$\left( \frac{v_{H_2}}{v_{NG}} \right) = \frac{\left( \frac{Z_{H_2}}{Z_{NG}} \right)}{\left( \frac{[HHV]_{H_2}}{[HHV]_{NG}} \right) \left( \frac{P_{av,H_2}}{P_{av,NG}} \right) \left( \frac{\eta_{H_2}}{\eta_{NG}} \right)} \quad (5)$$

Equation (5) shows that there are four terms that affect how much more gas is needed when switching from natural gas to hydrogen, each given as a ratio:

1. Compressibility factors
2. Higher heating values (by mole)
3. Pipeline pressures (average)
4. Boiler efficiencies

We will look at each of these ratios and compare the relative magnitudes of their effects on the overall velocity ratio. Note that as this form uses the molar HHV, the effect of density has been confined to the compressibility factor.

#### 3.3. Compressibility factor

The compressibility factor,  $Z$ , of any gas is a quantitative measure of its non-ideal behaviour. The temperature dependence of  $Z$  for hydrogen, natural gas, and pure methane is shown in Figure 1. The dependence on pressure is very slight for the narrow pressure range present in the distribution system[13, 1].

In the distribution pipework the compressibility factor of hydrogen is nearly constant at 1.0003 and the compressibility factor of natural gas is 0.997 at 8°C[8]. This means that the ratio of compressibility factors is  $Z_{H_2}/Z_{NG} = 1.003$ . This is a very small effect that is potentially within the uncertainty of other parameters in equation (5).

<sup>1</sup> The thermophysical data used in the paper come from NIST[11] and also from the CoolProp project[12] which publishes the algorithms as open source code.

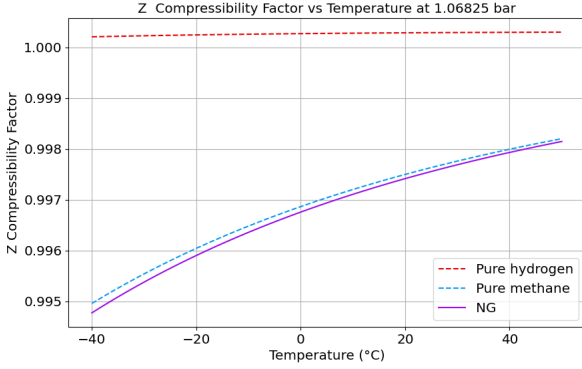


Figure 1: Plot of gas compressibility factors  $Z$ , showing the deviation from the ideal gas value of 1.0 calculated using the Peng-Robinson equation of state at 8°C[8].

### 3.4. Higher Heating Values [HHV]

Of these four terms, the HHV of the gases is the simplest as it is a molecular property that does not depend on the conditions of the gas. All Higher Heating Value data (Heat of Combustion) are by convention referred to a standard temperature and pressure of 25°C and 1 atm, i.e. close to room temperature. The HHV is the energy of the reaction in which the fuel and oxygen start at 25°C and 1 atm, are combusted, and then the sensible and latent heat of the combustion products is recovered as they are brought back down to 25°C and all the water is condensed[14]. The HHV of natural gas and hydrogen are shown in Table 2.

Table 2: Higher Heating Values at 25°C and 1 atm.

	HHV [kJ/mol]
H <sub>2</sub>	285.826
NG	940.813
ratio	0.304
reciprocal	3.292

A naive approximation to calculating the ratio of gas velocities may be made by assuming both gases to be close to ideal, the pressures close to atmospheric, and the boiler efficiencies to be the same for hydrogen and natural gas. Under these assumptions, then the velocity ratio would be equal to the reciprocal of the HHV ratio, as shown in Table 2 and the velocity of hydrogen required to supply the same quantity of heat would be  $3.292 \times$  that of natural gas. Previous studies have published a value of 3.13 for this velocity ratio, because they did not use the correct values for natural gas[1, 6]. The major cause of this difference is the approximately 7% by mole of longer hydrocarbons in UK natural gas that raise the molar HHV significantly compared to pure methane (Table 1).

### 3.5. Average pressure

The average pressure in the distribution network will depend on the pressure losses in the delivery of the gas

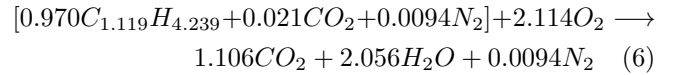
along the pipes, which in turn depends on the velocity of the gas. We are using the average pressure for natural gas as 40 mbar above atmospheric, but we require a value for hydrogen[10]. This requires an iterative solution procedure which will be performed in Section 5.4, so for now we simply state the result, that the average pressure for hydrogen is 45.88 mbar above atmospheric. Therefore the ratio of average pressures is  $P_{av,H_2}/P_{av,NG} = 1.0056$ .

### 3.6. Boiler efficiency

The efficiency of a domestic boiler is highly dependent on the design and operation of each individual unit. Rather than attempt to quantify the diverse array of domestic boilers which are in use in the UK, we will instead look at how the *maximum possible efficiency* differs for hydrogen and natural gas, and assume that the operation behaviour relative to this maximum efficiency is comparable for the two fuels. This means we are not considering gas velocity or heat transfer within the heat exchanger section of the boiler. We broadly categorise boilers into one of two different operating modes, those of a condensing or a non-condensing boiler.

- A non-condensing boiler vents the flue gas, the products of the combustion, with all of the water still in the gas phase.
- A condensing boiler attempts to recover latent heat by condensing some of the water vapour into liquid water.

The HHV is the absolute maximum energy that may be obtained from the fuel, when combusted under the conditions mentioned in Section 3.4, so the boiler efficiency  $\eta$  will be relative to the HHV[15]. Furthermore, as the fuel is not burned in pure oxygen, there is sensible heat lost to heating up the nitrogen in the air. Also a boiler will typically operate with 15% excess air, to ensure complete combustion of the fuel[16]. Any heat which is not recovered by not condensing water vapour, and inlet and outlet gases not at 25°C and 1 atm, is a reduction in efficiency[15].



The overall combustion reaction of one mole of the UK natural gas is given by equation (6), and the HHV of this reaction is 940.813 kJ/mol[14]. The list of reagents (fuel and air) and products of the combustion are shown in table 3. All of the combustible hydrocarbons may be combined into one pseudo-component[12] (see Appendix B), with a mole-averaged heat capacity of 37.276 kJ/mol·K[11] and the air is approximated as a mixture of 20.95% oxygen and 79.05% nitrogen<sup>2</sup>

<sup>2</sup>The weather-dependent humidity of the inlet air has an insignificant effect on the subsequent calculations, as does the small quantity of the pollutant  $NO_x$  produced in the combustion.

Table 3: NG combustion reaction in 15% excess air, with pseudo-component  $C_n H_m$  where  $n=1.119$  and  $m=4.239$ , and heat capacity  $C_P$  values[11] at 8°C and 1 atm.

Species	Reagents [mol]	Products [mol]	Products [mol/mol]	$C_p$ [J/mol·K]
$C_n H_m$	0.970			37.38
$O_2$	2.431	0.307	2.49%	36.28
$N_2$	9.181	9.181	73.99%	29.12
$CO_2$	0.021	1.140	8.94%	36.81
$H_2O$		2.119	16.61%	32.89 <sub>(g)</sub> 75.63 <sub>(l)</sub>

It can be seen that the flue gas from burning NG is rich in nitrogen (73.99%), with water as second highest fraction (16.61%). As water is the only condensable component in the flue gas<sup>3</sup>, the dew point of the mixture is the temperature at which the equilibrium vapour pressure of water is equal to its partial pressure[18]. In this mixture, 16.61% mole fraction of water corresponds to a partial pressure of 0.1661 atm, which is the vapour pressure of water[18] at 56.4°C (see Appendix C). This means that a boiler must cool the flue gas below this temperature for any condensation to occur.

As the representative temperature for a condensing boiler, we choose to use the recommended return flow temperature for central heating water of 50°C[19]. As we are neglecting inefficiencies in heat transfer within the boiler, the return flow temperature is taken to be equal to the flue gas exit temperature<sup>4</sup>. The equilibrium vapour pressure of water at 50°C is 0.1218 atm, and the partial pressure of water vapour in the flue gas is reduced to this value when 16.6% of the water present in the vapour has condensed out of the gas phase, leaving 72.4% of the water still as vapour. Under these conditions, there are four contributions to the loss of efficiency.

First, latent heat is required to evaporate 72.4% of the 2.119 moles of water. The heat of vaporisation of water at 25°C is 43.99 kJ/mol, which means that the latent heat lost in the boiler is 77.83 kJ/mol (per mole of NG).

Second, the natural gas in the distribution system is at 8°C, as mentioned in Section 2. Sensible heat is required to bring it up to 25°C, which are the conditions of the reagents according to definition of HHV. Using the heat capacity values from Table 2, heating the gas up to these conditions requires 0.522 kJ/mol. The variation of heat capacities with temperature is neglected for all species, due to the narrow temperature range being considered.

Third, the air will be at a different temperature to the natural gas. We assert that the best air temperature to use is the mean temperature weighted by gas use, i.e.

<sup>3</sup> Carbon dioxide may be neglected due to low solubility in water[17].

<sup>4</sup> The condensing temperature of the flue gas will not be the same as the water return temperature, as the heat exchanger is not infinitely long. A temperature difference of up to 5°C may be calculated from the efficiency values reported in[15, 20].

that temperature for which the amount of fuel burned in colder days matches that burned in warmer days. This is the mean temperature on a plot of daily fuel use against temperature on that day<sup>5</sup> and Terry and Galvin[21] model this as 5°C. Heating the air up to these conditions requires 6.77 kJ/mol (per mole of NG).

Lastly, the flue gas and condensed water is heated up from the 25°C, the conditions of the products according to the definition of HHV, to the exit temperature of 50°C. Heating the flue gas up to these conditions requires 9.40 kJ/mol (per mole of NG).

In total, this tells us that of the 940.8 kJ of HHV energy released from the combustion of one mole of NG, 95.55 kJ is lost, which is a maximum efficiency of  $\eta_{NG} = 89.95\%$  when the flue gas temperature is 50°C.

Now let us compare this to the combustion reaction for hydrogen, which is given by equation (7), and the HHV of this reaction is 285.8 kJ/mol. The list of reagents and products is shown in table 4.

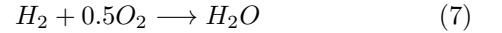


Table 4: Hydrogen combustion reaction in 15% excess air, with heat capacity  $C_P$ [11] at 8°C and 1 atm.

Species	Reagents [mol]	Products [mol]	Products [mol/mol]	$C_p$ [J/mol·K]
$H_2$	1			28.76
$O_2$	0.575	0.075	2.31%	29.34
$N_2$	2.170	2.170	66.87%	29.12
$H_2O$		1	30.82%	32.89 <sub>(g)</sub> 75.63 <sub>(l)</sub>

Comparing table 3 with table 4 we see that the flue gas from hydrogen combustion has nearly double the fraction of water than from combusting NG, 30.8% instead of 16.6%. This has the beneficial result that the partial pressure of water is higher, and thus that the dew point temperature is also higher at 70.0°C. Thus a pure-hydrogen condensing boiler does not need to run as cold to start recovering latent heat, and will recover more latent heat if operated at the same temperature than when using natural gas as the fuel. For the same representative 50°C flue gas temperature, the partial pressure of water in the flue gas is reduced to the equilibrium vapour pressure once 68.87% of the water vapour has been condensed out of the gas phase.

Repeating the same calculations that were performed for natural gas, the total sensible heat lost is 5.06 kJ/mol and the latent heat lost is 12.97 kJ/mol, both of which are per mole of hydrogen combusted. In total, this tells us that of the 285.8 kJ of HHV energy released from the combustion of one mole of hydrogen, 18.0 kJ is lost, which

<sup>5</sup>Ideally for boiler efficiency calculations this would be on an hourly basis, not a daily basis.

is a maximum efficiency of  $\eta_{H_2} = 93.7\%$  when the flue gas temperature is  $50^\circ\text{C}$ .

We conclude that a condensing boiler operating with a  $50^\circ$  flue gas temperature has a higher possible maximum efficiency when using hydrogen fuel than when using natural gas, as the higher dew point temperature means it is more easily able to recover heat by condensing water vapour out of the gas phase. Conversely, as there is a higher fraction of water vapour in the flue gas of a hydrogen boiler, if this heat is *not* recovered by condensation, such as by an imperfectly controlled boiler, then the efficiency *decreases* significantly.

These calculations<sup>6</sup> may be repeated for any specified flue gas exit temperature. If the temperature is above the dew point of the combustion then *all* of the latent heat of the water is lost. This data is plotted in Figure 2.

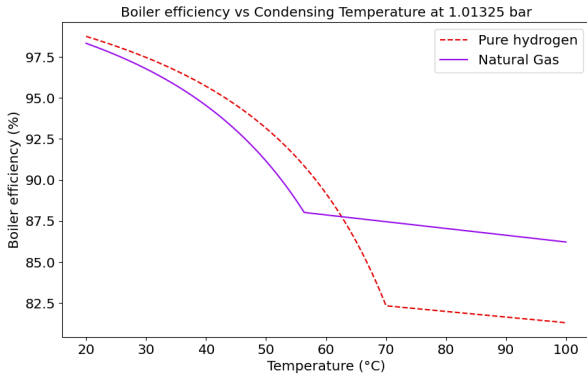


Figure 2: Maximum thermodynamic HHV efficiency of representative natural gas (blue) and hydrogen (red) combustion in 15% excess air as a function of the temperature to which the flue gas is cooled.

It can be seen that the lines for hydrogen and NG in Figure 2 intersect at  $63^\circ\text{C}$ . For a flue gas temperatures below this value, the hydrogen combustion has a *higher* maximum possible efficiency. For flue gas temperatures above this value, the hydrogen combustion has a *lower* maximum possible efficiency. The gradient of the efficiency curve above the dew point temperature<sup>7</sup> represents the sensible heat loss by the heat capacity of the flue gas: much of this is the energy required to heat the nitrogen in the inlet air.

For equation (5), we require a ratio of the two efficiencies. If we assume that all the existing boilers are condensing, and that all of them are perfectly adjusted with a flow temperature of  $50^\circ\text{C}$ , then the efficiency ratio would be  $\eta_{H_2}/\eta_{NG} = 1.027$ . This parameter is placed

<sup>6</sup> We have calculated dew points for 10 natural gas compositions, from Tokyo and the Netherlands to Algeria and the North Sea. The dew point temperatures range from  $56.03$  to  $58.8^\circ\text{C}$ [8].

<sup>7</sup>In some published versions of this boiler characteristic, if the line to the right of the dew point is horizontal, it means that those authors have not calculated the sensible heat loss. As this can be up to a third of the potential latent heat loss, any results in such a publication should be treated with caution.

on the denominator of equation (5), and so because hydrogen boilers are more efficient, the velocity ratio will be decreased by accounting for boiler efficiencies.

However, it is not sensible to assume that all existing boilers operate this optimally. We have data on how many piped-gas boilers in the UK are condensing, but we would need to make an assumption as to how this would change after conversion to pure hydrogen boilers. Current regulations[22] are that all new boilers must be condensing, so the population boiler efficiency ratio will change substantially purely from this, without including the extra benefit from having a higher-efficiency fuel. In addition, it is highly doubtful that all current condensing boilers are correctly set with a return flow temperature of  $50^\circ\text{C}$  whereas it is more likely that more of the new hydrogen boilers would be configured correctly. Appendix D calculates that an appropriate overall efficiency multiplier using 2022 data would be  $\eta_{H_2}/\eta_{NG} = 1.067$ .

### 3.7. Velocity ratio

Combining all of terms that have been calculated for equation (5) gives us, from equation (8), a value of 3.076 for the ratio of the velocities of hydrogen to natural gas through the same pipes.

- The ratio of compressibilities is 1.003, indicating that hydrogen is less dense than natural gas on a molar basis.
- The ratio of HHVs is 0.304, indicating that hydrogen produces significantly less energy when combusted than natural gas, on a molar basis.
- The ratio of average pressures is 1.0056. This value is determined iteratively from the velocity ratio in Section 5.4.
- The ratio of boiler efficiencies is 1.067, indicating that condensing boilers burning hydrogen combustion are more efficient than those burning natural gas.

$$\left( \frac{v_{H_2}}{v_{CH_4}} \right) = \frac{1.003}{0.304 \times 1.0056 \times 1.067} = \mathbf{3.076} \quad (8)$$

This velocity ratio is very close to the reciprocal of the molar HHV ratio. The compressibility ratio and average pressure ratio each contribute less than 1% change to the velocity ratio. The largest secondary effect is the efficiency of condensing boilers.

These are the values for the Fordoun natural gas. We have also run the same calculations with other gas mixtures and there is no substantive difference in the results (details are listed in the software[8]).

#### 4. UK gas distribution network

Transmission natural gas networks<sup>8</sup> are designed to run in fully-turbulent mode at peak design flow, with gas velocities in the range 8-12 m/s. A general guideline for all gas networks is that the gas velocity should be between 5 and 10 m/s and always less than 20 m/s to prevent erosive wear by dust particles[23, 24, 25].

##### 4.1. UK service pipes

In the UK *distribution* grid at the point of connection to a domestic residence, the pressure is between 75 mbar and 20 mbar above atmospheric pressure.

The domestic gas demand is the “Service Pipe Energy Value”. Gas appliances in the UK within the household are typically designed to expect an input pressure of 20 mbar<sup>9</sup>.

A typical household in the UK will have a gas meter capable of reading flows up to 6 m<sup>3</sup>/hour (71 kW in HHV). For a typical 35mm diameter gas pipe, this is a gas velocity of 1.73 m/s. The gas velocity will be always lower than this as most household central heating boilers are 20 kW or less.

#### 5. Flow through pipes

We need a way of comparing the flow of hydrogen with the flow of natural gas through a pipe. There is a wide choice of apparently useful equations<sup>10</sup> available in the gas industry, but almost none are correct for hydrogen and few describe the range of flow regimes we need to understand.

We need to take a more fundamental approach. At the low pressure and narrow pressure range present in the distribution grid, the incompressible fluid approximation is accurate[18], so we should use the Darcy-Weisbach equation for the pressure drop along a pipe:

$$\Delta p = f \left( \frac{L}{D} \right) \frac{1}{2} \rho v^2 \quad (9)$$

where  $L$  is the length of the pipe,  $D$  the diameter of the pipe,  $v$  is the mean velocity of the gas,  $\rho$  the density, and  $f$  the Darcy friction factor.

The Darcy friction factor is a dimensionless parameter that determines the resistance to flow. It depends on the type of flow, or regime, that the fluid experiences.

The different flow regimes are separated by the relative importance of inertial and viscous forces. The ratio of

<sup>8</sup>Numerical evidence is from the Netherlands[23] as UK gas network data is now redacted by the regulator.

<sup>9</sup>The operating pressure of the outlet of the gas meter “should not be less than 18.5 mbar and not more than 23 mbar” [26].

<sup>10</sup> Weymouth, Panhandle A, Panhandle B, Spitzglass, various ‘power laws’, Colebrook[27]. Many of these are dimensionally inhomogeneous and use ‘industry units’ where conversion factors are embedded in the equation constants, or where the range of applicability is not at all obvious to the user.

these two behaviours is the Reynolds number,  $Re$ , which also serves as a dimensionless form of the velocity:

$$Re = \left( \frac{\rho v D}{\mu} \right) \quad (10)$$

where  $\mu$  is the dynamic viscosity in Pa s.

Experimental results have shown that  $f$  always takes a value between 0.007 and 0.1, however its dependence on the Reynolds number is somewhat complex [28], and also depends on the pipe roughness.

##### 5.1. Flow regimes

It is helpful to visualise the flow of fluids through pipes with the Moody diagram, see Figure 3. This relates the friction factor  $f$  against the Reynolds number  $Re$  and the pipe roughness  $\epsilon/D$ , where  $\epsilon$  is the absolute pipe roughness in m and  $D$  is the diameter of the pipe in m. This shows three regimes with different flow behaviour.

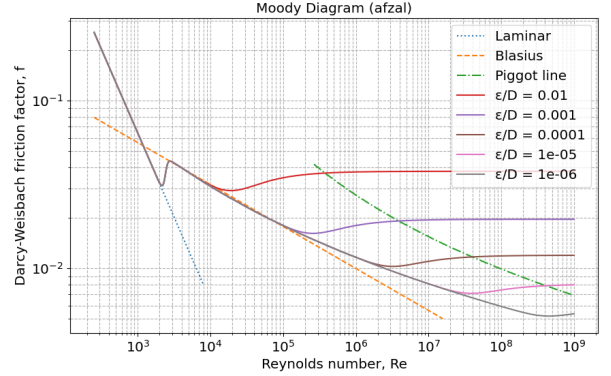


Figure 3: Moody diagram showing the friction factor as a function of the Reynolds number. The Piggot line marks the transition between inflectional- and fully-turbulent behaviour[29]. We use the Afzal equation[30] for the lines of different roughness as this is algebraically the most convenient of several which match the inflectional Nikuradze behaviour[28, 31]

1. At the left-hand side of the Moody diagram is the laminar regime, which follows the analytical result of the Hagen-Poiseuille equation regardless of the roughness of the pipe (dotted line).
2. In the middle, between the laminar line (dotted) and the Piggot line (dash-dotted) there is the partially-turbulent regime. Most real gas distribution pipes operate in this regime.
3. At the right-hand side is the fully-turbulent regime, in which the friction factor depends only on roughness, and is independent of  $Re$  (horizontal lines to the right of the Piggot line).

##### 5.2. Regime in the service pipe

A typical domestic connection to the distribution network in the UK is a 35 mm tube of drawn copper, steel, or polyethylene[1]. A typical domestic boiler in the UK is



rated at 30 kW[22, 32]. The energy supply equation (4), as well as the material properties used in Section 3.7, allows us to calculate that the gas velocity of natural gas in this situation is  $v=0.838$  m/s, and the Reynolds number is  $Re=2363$ . This places the flow at the upper-left of the partially-turbulent regime, see Figure 3.

Replacing natural gas with hydrogen in any piping system will always reduce the Reynolds number, because while the velocity increases, the density decreases significantly more, and the dynamic viscosity of also decreases<sup>11</sup>. See Section 5.7 for these calculations.

Calculating the Reynolds number for this situation with pure hydrogen gives a value of at 970, quite definitely in the laminar flow regime where the pressure drop is linear in velocity. Therefore we need to consider multiple regimes that are applicable to different sections of the distribution network.

### 5.3. Partially-turbulent flow

The partially-turbulent regime in Figure 3 is between the laminar flow line and the Piggot line<sup>12</sup>, determined by equation 11. Most of the UK gas distribution network would appear to be in this regime [Citation Needed].

$$\frac{3500}{\epsilon/D} = Re \quad (11)$$

The ‘gap’ visible in figure 3 between the laminar line at  $Re = 2 \times 10^2$  and merged curves representing varying pipe-roughness is where the flow transitions from laminar to turbulent[31]. The difference in values of  $f$  across this gap may be as low as 0.02, in specifically prepared test specimens, or as high as 0.06.

The full dependence of the friction factor on  $Re$  and the relative roughness of the pipe for all fluids in pipes may be determined from the underlying physics by the Goldenfeld function[28, 31, 33].

Figure 3 shows lines for pipes of different roughnesses<sup>13</sup> by use of equation M.7, for relative roughness values of  $10^{-2}$ ,  $10^{-3}$ ,  $10^{-4}$ , and  $10^{-5}$ . Smooth pipes are defined as those where  $\epsilon/D < 10^{-5}$ , for which the gas flow is partially-turbulent for  $Re < 10^5$ .

<sup>11</sup>We use a simple molar fraction weighted approximation for the viscosity of gas mixtures, as that is adequate for the purpose of this paper. For modelling higher pressure transmission networks, a much more complex Chapman-Enskog or corresponding states[12] model would be required.

<sup>12</sup>Piggot observed this relationship between  $Re$  and relative roughness ( $\epsilon/D$ ) which is the point at which fully turbulent flow develops. It was first reported in the discussion published at the end of the original Moody paper[29]. For large diameter drawn tubing with ( $\epsilon/D$ ) =  $5 \cdot 10^{-6}$  this transition is at  $Re = 7 \cdot 10^8$ .

<sup>13</sup>There are at least 50 different semi-empirical equations which approximate the implicit Colebrook equation but these are simply mathematical fits and ignore the fact that the Colebrook equation itself does not describe experimental data from very smooth pipes[28, 30, 33]. All calculations on natural gas and hydrogen use the Blasius equation[8].

Table 5: Densities and dynamic viscosities at 8°C and 1 atm

	Density [kg/m <sup>3</sup> ]	Dynamic viscosity [μPa s]
H <sub>2</sub>	0.0914	8.509
NG	0.0836	10.374
ratio	0.1902	0.8202

Behaviour in the partially-turbulent regime may be further subdivided. At the lower end of Reynolds number the behaviour asymptotically approaches the Blasius law, shown in Figure 3 as a dashed straight line. The friction factor  $f$  in this Blasius sub-regime is given by equation 9[34].

$$f_{Blas} = 0.079 \times Re^{-1/4} \quad (12)$$

For smooth pipes, such as steel or polyethylene with a relative roughness of  $10^{-5}$ , the friction factor  $f$  for gas in distribution pipes is always between 0.008 and 0.045, as can be seen from Figure 3. For  $Re$  less than  $2 \times 10^5$  the friction factor follows the Blasius law, for more than  $2 \cdot 10^5$  it diverges[28] but still depends on  $Re$  until about  $3 \cdot 10^8$ <sup>14</sup>.

### 5.4. Pressure drop in the Blasius sub-regime

Bossel [6] calculated the ratios of pressure drop and pumping power for hydrogen as compared to methane. Here we extend his analysis by using the in depth velocity ratio from Section 3.7, and accounting for the fact that the friction factor changes with velocity in the regimes present in the distribution system. Instead of using the complete Afzal or Goldenfeld equations, we will use the Blasius equation, which restricts our range of applicable Reynolds numbers to  $Re \in (2 \times 10^3, 2 \times 10^5)$ .

We can combine the Darcy-Weisbach equation (9), the Blasius equation (12), and the Reynolds number definition (10), to give the dependence of pressure drop on all relevant parameters:

$$\Delta P = \left( \frac{4 \cdot 0.079}{D^{5/4}} \right) \cdot \rho^{3/4} \cdot \mu^{1/4} \cdot v^{7/4} \quad (13)$$

The terms in brackets of equation (13) are constant when comparing any fluids in the same pipe. The remaining terms show the dependency on material properties, given in table 5, and the gas velocity. The combined material parameter  $\rho^{3/4} \times \mu^{1/4}$  has interesting temperature dependence, see Appendix E.2. We can take the ratio of this equation for the two fuels to give equation (14).

$$\left( \frac{\Delta P_{H_2}}{\Delta P_{NG}} \right)_{Blasius} = \left( \frac{\rho_{H_2}}{\rho_{NG}} \right)^{3/4} \left( \frac{\mu_{H_2}}{\mu_{NG}} \right)^{1/4} \left( \frac{v_{H_2}}{v_{NG}} \right)^{7/4} \quad (14)$$

<sup>14</sup>This dependence is a characteristic of the physics of critical systems as shown by Goldenfeld [31].

Unlike equation (5) for the velocity ratio, equation (14) directly includes the density,  $\rho$ , as it is an important factor in the inertial forces giving rise to pressure drop. Using the material properties from table 5 and the velocity ratio from 3.7 for hydrogen and natural gas, we find the ratio of pressure drops of the two gases to be:

$$\left(\frac{\Delta P_{H_2}}{\Delta P_{NG}}\right) = 0.1902^{3/4} \times 0.8202^{1/4} \times 3.076^{7/4} = \mathbf{1.294} \quad (15)$$

Now that we can calculate the pressure drop from the velocity, we can perform the iterative calculations to work out the average pipe pressure that was used in Section 3.5. The distribution network is controlled such that the low pressure end is kept at 20 mbar (gauge)[1], and we have been using an average pressure for natural gas of 40 mbar (gauge)[10]. Thus, the pressures in this idealised distribution pipe are 60 mbar inlet to 20 mbar outlet, with a 40 mbar pressure drop.

Upon switching to hydrogen, this 40 mbar drop is increased by  $1.294\times$  to become 51.75 mbar. With the outlet kept at 20 mbar gauge, this requires that the inlet is increased to 71.75 mbar, which is within the maximum of 75 mbar gauge that the distribution network is rated to contain[1]. The average of these inlet and outlet pressures is 45.88 mbar, which is the value that was used in Section 3.5, showing that this value is the converged result of the iterative calculation.

### 5.5. Compressor power

The pressure drop of a flowing fluid arises from frictional losses, and the pumping power,  $W$ , required to overcome these losses for an incompressible fluid is the product of the pressure drop and the volumetric flow rate. For flow in a pipe this may be calculated by:

$$W = \Delta P \cdot v \cdot A \quad (16)$$

The proportional increase in the compression power requirement when switching from natural gas to hydrogen is therefore the ratio of this equation for the two gases:

$$\left(\frac{\Delta P_{H_2}}{\Delta P_{NG}}\right)_{Blas} = \left(\frac{\rho_{H_2}}{\rho_{NG}}\right)^{3/4} \left(\frac{\mu_{H_2}}{\mu_{NG}}\right)^{1/4} \left(\frac{v_{H_2}}{v_{NG}}\right)^{7/4} \quad (17)$$

Note that this expression also uses the combined material parameter  $\rho^{3/4} \times \mu^{1/4}$  that was present in equation 13.

$$\left(\frac{W_{H_2}}{W_{NG}}\right)_{Blas} = 0.1902^{3/4} \times 0.8202^{1/4} \times 3.076^{11/4} = \mathbf{3.980} \quad (18)$$

This value tells us that the energy required to deliver hydrogen through the distribution network will be  $3.98\times$  greater than for natural gas, if the flow remains in the Blasius part of the partially-turbulent regime. At higher Reynolds numbers, the friction factor should be calculated using a more widely applicable equation.

### 5.6. Limiting regimes

Below a Reynolds number of  $2 \times 10^3$ , all pipes regardless of roughness should exhibit laminar behaviour. The friction factor in this regime can be expressed analytically from the Hagen-Poiseuille equation as:

$$f_{Lam} = \frac{16}{Re} \quad (19)$$

This may be used in place of equation (12) to expressions for the pressure drop ratio and the compressor power ratio in the laminar regime with different exponents on the 3 terms:

$$\left(\frac{\Delta P_{H_2}}{\Delta P_{NG}}\right)_{Lam} = \left(\frac{\rho_{H_2}}{\rho_{NG}}\right)^0 \left(\frac{\mu_{H_2}}{\mu_{NG}}\right)^1 \left(\frac{v_{H_2}}{v_{NG}}\right)^1 = \mathbf{2.523} \quad (20)$$

$$\left(\frac{W_{H_2}}{W_{NG}}\right)_{Lam} = \left(\frac{\rho_{H_2}}{\rho_{NG}}\right)^0 \left(\frac{\mu_{H_2}}{\mu_{NG}}\right)^1 \left(\frac{v_{H_2}}{v_{NG}}\right)^2 = \mathbf{7.763} \quad (21)$$

At sufficiently high Reynolds number, flow enters the fully turbulent regime where  $f$  is independent of  $Re$ . For smooth pipes of  $\epsilon/D = 10^{-5}$ , the limit is  $Re = 3 \times 10^8$  and the limiting value is  $f_{FT} = 0.009$ . This may be also used in place of equation (12) to derive expressions for the ratios in the fully turbulent regime:

$$\left(\frac{\Delta P_{H_2}}{\Delta P_{NG}}\right)_{FT} = \left(\frac{\rho_{H_2}}{\rho_{NG}}\right)^1 \left(\frac{\mu_{H_2}}{\mu_{NG}}\right)^0 \left(\frac{v_{H_2}}{v_{NG}}\right)^2 = \mathbf{1.035} \quad (22)$$

$$\left(\frac{W_{H_2}}{W_{NG}}\right)_{FT} = \left(\frac{\rho_{H_2}}{\rho_{NG}}\right)^1 \left(\frac{\mu_{H_2}}{\mu_{NG}}\right)^0 \left(\frac{v_{H_2}}{v_{NG}}\right)^3 = \mathbf{3.185} \quad (23)$$

### 5.7. General relationships

While the three sets of values derived work well for cases in which the fluid regime is well defined, there are gaps between these regimes. The transition from laminar to partially turbulent behaviour is notoriously complex, however recent works have made an effort to understand this transition on a fundamental level [Citation needed]. There is also a wide section of the partially-turbulent regime from  $Re = 2 \times 10^5$  to  $3.5 \times 10^8$  where the friction factor is not yet constant but also does not follow the Blasius equation. It appears that much of the UK gas grid, including many of the high pressure transmission pipelines, are in this non-Blasius sub-regime [Citation needed].

Furthermore, replacing natural gas with hydrogen also affects the Reynolds number. In the service pipe mentioned in Section 5.2, the regime was partially turbulent with natural gas, yet switching to hydrogen resulted in



laminar flow. For the average gas velocity change of  $3.076\times$  from natural gas to hydrogen, there is a Reynolds' number shift which depends on the relative velocity changes and also on the relative densities of hydrogen and natural gas:

$$\left(\frac{Re_{H_2}}{Re_{NG}}\right) = \frac{\left(\frac{\rho_{H_2}}{\rho_{NG}}\right)\left(\frac{v_{H_2}}{v_{NG}}\right)}{\left(\frac{\mu_{H_2}}{\mu_{NG}}\right)} = \mathbf{0.4103} \quad (24)$$

The laminar, Blasius, and fully turbulent regimes serve as limiting cases for the values of the pressure drop and compressor power ratios across any regime. For the service pipe mentioned in Section 5.2, the regime changes from Blasius to laminar, so we should expect the increase in compressor power required to increase by a value between 7.763 (laminar) and 3.980 (Blasius).

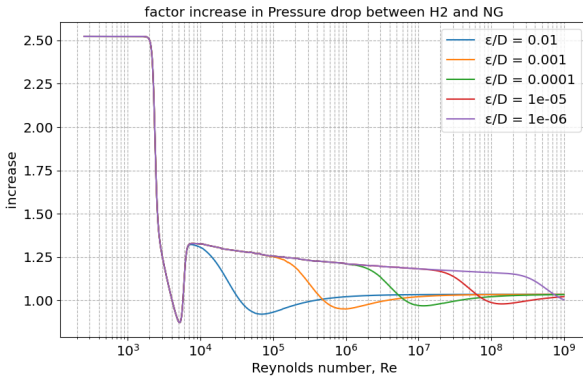


Figure 4: The factor increase curve is the same shape both for pressure drop and compressor power when replacing natural gas with hydrogen as the velocity ratio is always 3.076; when the friction factor is calculated independently.

A fortunate consequence is that these values decrease as the Reynolds number increase, thus the largest increases to the pressure and compressor power occur at the locations where the flow is already slow, and thus have the lowest pressures and frictional losses. This is similar to the existing situation, where during off-peak demand hours the gas velocity drops and the Reynolds number drops. This decrease in  $Re$  means an increase in  $f$ , however the reduction in velocity means that the power requirement overall drops.

The increase in the compression power for hydrogen over natural gas has been noted by Schouten[23] and others, but only for fully-turbulent conditions. The increase in friction factor and the consequent further increase in compressor power required has not previously been recognised.

## 6. UK distribution capabilities

Although the standard maximum pressure for the Low Pressure (LP) distribution grid is 75 mbar much of the older network runs at only 50 mbar[2] to reduce leakage,

where this still gives adequate pressure (20 mbar) at the most distant user. This could be increased up towards the maximum 75 mbar level with new polyethylene pipe which is less prone to leaks[2]. Also, in 2023 there is new technology available to automatically vary the pressure at the governors at the higher-pressure end of the LP pipes such that it is as low as possible, consistent with good service[10]. There are more than 26,000 of these governors in the UK network and the majority of them are currently set manually or by clock mechanisms. Thus recent technology developments are expected to ease considerably the management of a 100% hydrogen service with existing pipes.

The UK domestic gas demand[35] peaked in 2004 at 34,035 toe (tonne of oil equivalent, 1 toe is equal to 10 MWh and in the most recent cold winter year (2021) it was 26,275 toe. So the network today can cope with an annual demand at least 29.5% higher than it currently supplies. While it is possible that during the peak hourly demands of 2004 and 2021 this ratio was less than the annual ratio, we can only expect that this over-capacity will continue to grow into the future as more houses get insulated, upgraded or replaced and also due to climate change reducing the heating demand overall[36].

### 6.1. Other factors

Distributing hydrogen has other complexities that this paper does not address. These include maintaining the required concentration[3], Joule-Thompson cooling and the effects of retrograde liquid dropout[23], compressor issues[37], compatibility with tanks in CNG vehicles[38] and linepack[39].

## 7. Conclusions

While it is clear that burning hydrogen for heat in a boiler, or even in a combined heat and power cell, is almost a use of last resort[40, 41], there appear to be no pressure difficulties with delivering pure hydrogen using the existing UK distribution network. The calculations in this paper show that the velocity is similar to that which had previously been thought but that the pressure drop and power requirement are higher.

It has not previously been noted that

- burning hydrogen means that care must be taken to reduce the condensation temperature of the condensing boiler as much as possible because a greater proportion of the combustion energy is in the form of condensable water,
- converting from natural gas to hydrogen reduces the Reynolds' number of the flow rather than increasing it,
- there is a slight effect of increasing the mean pressure, and thus the energy density, of the hydrogen because it requires a 29% higher pressure gradient to be delivered, or that

- the Blasius material parameter  $\rho^{3/4} \cdot \mu^{1/4}$  has a very low temperature dependence. This means that our conclusions on relative pressure drop and the relative compression power are insensitive to temperature where the Blasius correlation holds.

As well as the low pressure system investigated here, it is likely that the Medium and Intermediate Pressure distribution pipes are operating for much of the time in the partially-turbulent regime.

## 8. References

- [1] P. Dodds, S. Demoullin, Conversion of the uk gas system to transport hydrogen, *International Journal of Hydrogen Energy* 38 (18) (2013) 7189–7200.  
URL <http://dx.doi.org/10.1016/j.ijhydene.2013.03.070>
- [2] ARUP, Future of great britain's gas networks - final report for national infrastructure commission and ofgem (2023).  
URL <https://nic.org.uk/app/uploads/Arup-Future-of-UK-Gas-Networks-18-October-2023.pdf>
- [3] NationalGrid, Hydrogen blends in the nts - a theoretical exploration gas future operability planning (2021).  
URL <https://www.nationalgas.com/document/137506/download>
- [4] NationalGas, Gas ten year statement network capability (2023).  
URL <https://www.nationalgas.com/insight-and-innovation/gas-ten-year-statement-gtys>
- [5] S. Samsatli, N. J. Samsatli, The role of renewable hydrogen and inter-seasonal storage in decarbonising heat comprehensive optimisation of future renewable energy value chains, *Applied Energy* 233-234 (2019) 854–893. doi:10.1016/j.apenergy.2018.09.159.
- [6] U. Bossel, Does a hydrogen economy make sense?, *Proceedings of the IEEE* 94 (10) (2006) 1826–1836. doi:10.1109/JPROC.2006.883715.  
URL [https://www.researchgate.net/publication/2998127\\_Does\\_a\\_Hydrogen\\_Economy\\_Make\\_Sense](https://www.researchgate.net/publication/2998127_Does_a_Hydrogen_Economy_Make_Sense)
- [7] cngservices, Fordoun case study (2019).  
URL [https://www.cngservices.co.uk/case\\_study/fordoun/](https://www.cngservices.co.uk/case_study/fordoun/)
- [8] P. Sargent, M. Sargent, Hydrogen in pipes - software (Dec. 2023). doi:10.5281/zenodo.10368611.  
URL <https://github.com/PhilipSargent/h2-in-pipes>
- [9] D. J. C. MacKay, Sustainable Energy - Without the Hot Air, UIT Cambridge Ltd., 2008, Ch. E Heating II, pp. 303–304.  
URL [https://www.withouthotair.com/cE/page\\_303.shtml](https://www.withouthotair.com/cE/page_303.shtml)
- [10] UTONOMY, Utonomys pressure management (2023).  
URL <https://utonomy.co.uk/case-studies/2023/04/utonomys-smart-gas-solution-helps-sgn-reduce-pressure-leakage-and-costs-in-henley-on-thames/>
- [11] M. L. Huber, E. W. Lemmon, I. H. Bell, M. O. McLinden, The nist refprop database for highly accurate properties of industrially important fluids (10 2022). doi:10.1021/acs.iecr.2c01427.  
URL <https://webbook.nist.gov/cgi/cbook.cgi>
- [12] I. H. Bell, J. Wronski, S. Quoilin, V. Lemort, Pure and pseudo-pure fluid thermophysical property evaluation and the open-source thermophysical property library coolprop, *Industrial & Engineering Chemistry Research* 53 (6) (2014) 2498–2508. arXiv:<http://pubs.acs.org/doi/pdf/10.1021/ie4033999>, doi:10.1021/ie4033999.  
URL <http://pubs.acs.org/doi/abs/10.1021/ie4033999>
- [13] S. 284, The gas safety (management) (amendment) regulations 2023 (3 2023).
- [14] D. R. Burgess, A. P. Hamins, Technical Note Heats of Combustion and Related Properties of Pure Substances Heats of Combustion and Related Properties of Pure Substances, NIST, 2023.
- [15] H. Satyavada, S. Baldi, Monitoring energy efficiency of condensing boilers via hybrid first-principle modelling and estimation, *Energy* 142 (2018) 121–129. doi:10.1016/j.energy.2017.09.124.
- [16] Cleaver-Books, The impact of excess air on efficiency (9 2016).  
URL <https://www.watmfg.com/watmfg23082016/wp-content/uploads/2016/09/Excess-Air-and-Boiler-Efficiency.pdf>
- [17] Y. Zhao, H. Diao, Y. Qin, L. Xie, M. Ge, Y. Wang, S. Wang, Effect of flow rate on condensation of CO<sub>2</sub>-water vapor mixture on a vertical flat plate, *Applied Thermal Engineering* 229 (2023) 120557. doi:<https://doi.org/10.1016/j.applthermaleng.2023.120557>.  
URL <https://www.sciencedirect.com/science/article/pii/S1359431123005860>
- [18] R. H. Perry, D. W. Green, J. O. Maloney, Perry's Chemical Engineers' Handbook, 8th Edition, McGraw-Hill, 2008.  
URL <https://api.semanticscholar.org/CorpusID:56182942>
- [19] BEIS, Review of the methodology for fghrs in sap final report (2021).  
URL <https://assets.publishing.service.gov.uk/media/614b218ee90e077a2db2e793/review-methodology-fghrs-sap.pdf>
- [20] DESNZ, Lab testing - boiler cycling (12 2023).  
URL <https://assets.publishing.service.gov.uk/media/65785a000467eb000d55f5ce/hem-val-05-lab-testing-boiler-cycling.pdf>
- [21] N. Terry, R. Galvin, How do heat demand and energy consumption change when households transition from gas boilers to heat pumps in the UK, *Energy and Buildings* 292 (2023) 113183. doi:10.1016/j.enbuild.2023.113183.  
URL <https://linkinghub.elsevier.com/retrieve/pii/S0378778823004139>
- [22] G. Orr, T. Lelyveld, BurtonSimon, Final report: In-situ monitoring of efficiencies of condensing boilers and use of secondary heating (6 2009).  
URL [https://assets.publishing.service.gov.uk/media/5a75149be5274a3cb28697f7/In-situ\\_monitoring\\_of\\_condensing\\_boilers\\_final\\_report.pdf](https://assets.publishing.service.gov.uk/media/5a75149be5274a3cb28697f7/In-situ_monitoring_of_condensing_boilers_final_report.pdf)
- [23] J. A. Schouten, J. P. J. Michels, R. J. van Rosmalen, Effect of h<sub>2</sub>-injection on the thermodynamic and transportation properties of natural gas, *International Journal of Hydrogen Energy* 29 (2004) 1173–1180.  
URL <https://www.sciencedirect.com/science/article/abs/pii/S0360319903003112>
- [24] F. Tabkhi, C. AzzaroPantel, L. Pibouleau, S. Domenech, A mathematical framework for modelling and evaluating natural gas pipeline networks under hydrogen injection, *International Journal of Hydrogen Energy* 33 (2008) 6222–6231.  
URL <https://www.sciencedirect.com/science/article/abs/pii/S0360319908009634>
- [25] E. K. Ejomarie, E. G. Saturday, Optimal design of gas pipeline transmission network, *Global Scientific Journals* 8 (2020) 918–938.  
URL [www.globalscientificjournal.com](http://www.globalscientificjournal.com)
- [26] IGEN, Domestic supply capacity and operating pressure at the outlet of the meter (2023).  
URL <https://bit.ly/47scx58>
- [27] D. Brkić, P. Praks, Unified Friction Formulation from Laminar to Fully Rough Turbulent Flow, *Applied Sciences*.  
URL <https://api.semanticscholar.org/CorpusID:53476706>
- [28] J. J. Allen, M. A. Shockling, G. J. Kunkel, A. J. Smits, Turbulent flow in smooth and rough pipes, *Philosophical Transactions of the Royal Society A: Mathematical, Physical and Engineering Sciences* 365 (1852) (2007) 699–714. doi:10.1098/rsta.2006.1939.
- [29] L. Moody, Friction factors for pipe flow, *Transactions of the ASME* 66 (1944) 671–684.
- [30] R. T. Cerbus, C. C. Liu, G. Gioia, P. Chakraborty, Laws of Resistance in Transitional Pipe Flows, *Physical Review Letters* 120 (5) (2018) 54502. doi:10.1103/PhysRevLett.120.054502.  
URL <https://doi.org/10.1103/PhysRevLett.120.054502>

- [31] N. Goldenfeld, Roughness-induced critical phenomena in a turbulent flow, *Physical Review Letters* 96 (4) (2006) 1–4. [arXiv:0509439](#), [doi:10.1103/PhysRevLett.96.044503](#).
- [32] G. Bennett, C. Elwell, Effect of boiler oversizing on efficiency: a dynamic simulation study, *Building Services Engineering Research and Technology* 41 (6) (2020) 709–726. [doi:10.1177/0143624420927352](#).
- [33] Z. S. She, Y. Wu, X. Chen, F. Hussain, A multi-state description of roughness effects in turbulent pipe flow, *New Journal of Physics* 14. [doi:10.1088/1367-2630/14/9/093054](#).
- [34] C. A. Bennett, R. P. Hohmann, Methods for calculating shear stress at the wall for single-phase flow in tubular, annular, plate, and shell-side heat exchanger geometries, *Heat Transfer Engineering* 38 (2017) 829–840. [doi:10.1080/01457632.2016.1211913](#).  
URL <https://doi.org/10.1080/01457632.2016.1211913>
- [35] DESNZ, *Ecuk 2023: End uses data tables (excel)* (9 2023).  
URL <https://www.gov.uk/government/statistics/energy-consumption-in-the-uk-2023>
- [36] N. Christidis, M. McCarthy, P. A. Stott, Recent decreases in domestic energy consumption in the united kingdom attributed to human influence on the climate, *Atmospheric Science Letters* 22. [doi:10.1002/asl.1062](#).
- [37] A. Witkowski, A. Rusin, M. Majkut, K. Stolecka, Analysis of compression and transport of the methane/hydrogen mixture in existing natural gas pipelines, *International Journal of Pressure Vessels and Piping* 166 (2018) 24–34. [doi:10.1016/j.ijpvp.2018.08.002](#).  
URL <https://www.sciencedirect.com/science/article/pii/S0308016118301698>
- [38] K. Altfeld, D. Pinchbeck, Admissible hydrogen concentrations in natural gas systems (2013).  
URL [www.gas-for-energy.comhttps://www.gerg.eu/wp-content/uploads/2019/10/HIPS\\_Final-Report.pdf](http://www.gas-for-energy.comhttps://www.gerg.eu/wp-content/uploads/2019/10/HIPS_Final-Report.pdf)
- [39] M. Witek, F. Uilhoorn, Impact of hydrogen blended natural gas on linepack energy for existing high pressure pipelines, *Archives of Thermodynamics* 43 (2022) 111–124. [doi:10.24425/ather.2022.143174](#).
- [40] J. Rosenow, A meta-review of 54 studies on hydrogen heating, *Cell Reports Sustainability* (2023) 100010 [doi:10.1016/j.crsus.2023.100010](#).
- [41] M. Liebreich, The clean hydrogen ladder [now updated to v4.1] - liebreich (8 2021).  
URL <https://www.liebreich.com/the-clean-hydrogen-ladder-now-updated-to-v4-1/>
- [42] D. Lozano-Martn, A. Moreau, C. R. Chamorro, Thermophysical properties of hydrogen mixtures relevant for the development of the hydrogen economy: Review of available experimental data and thermodynamic models, *Renewable Energy* 198 (2022) 1398–1429. [doi:10.1016/j.renene.2022.08.096](#).  
URL <https://www.sciencedirect.com/science/article/pii/S096014812201271X>
- [43] A. Pina-Martinez, R. Privat, J.-N. Jaubert, D.-Y. Peng, Updated versions of the generalized soave  $\phi$ -function suitable for the redlich-kwong and peng-robinson equations of state, *Fluid Phase Equilibria* 485 (2019) 264–269. [doi:10.1016/j.fluid.2018.12.007](#).
- [44] DLUHC, English housing survey 2021 to 2022: headline report (2022).  
URL <https://bit.ly/3Hf4q0v>
- [45] F. J. Krieger, Calculation of the Viscosity of Gas Mixtures, Tech. rep., RAND Corporation (1951).  
URL [https://www.rand.org/pubs/research\\_memoranda/RM649.html](https://www.rand.org/pubs/research_memoranda/RM649.html)
- [46] ISO, Iso 13443:1996 natural gas standard reference conditions (2020).  
URL <https://www.iso.org/standard/20461.html>
- [47] D. Lander, T. Humphreys, The revision of iso-6976 and assessment of the impacts of changes, from UK gas governance website. (2017).  
URL [https://bit.ly/IS06976\\_commentary](https://bit.ly/IS06976_commentary)
- [48] R. Privat, J. N. Jaubert, The state of the art of cubic equations of state with temperature-dependent binary interaction coefficients: From correlation to prediction, *Fluid Phase Equilibria* 567. [doi:10.1016/j.fluid.2022.113697](#).
- [49] J. J. Carroll, J. D. Slupsky, A. E. Mather, The solubility of carbon dioxide in water at low pressure, *Journal of Physical and Chemical Reference Data* 20 (1991) 1201–1209. [doi:10.1063/1.555900](#).  
URL <https://doi.org/10.1063/1.555900>
- [50] G. Gioia, P. Chakraborty, Turbulent friction in rough pipes and the energy spectrum of the phenomenological theory, *Physical Review Letters* 96 (4) (2006) 1–4. [arXiv:0507066](#), [doi:10.1103/PhysRevLett.96.044502](#).
- [51] T. P. Brackbill, S. G. Kandlikar, Effects of low uniform relative roughness on single-phase friction factors in microchannels and minichannels, in: *Proceedings of the 5th International Conference on Nanochannels, Microchannels and Minichannels, ICNMM2007*, 2007, pp. 509–518, january 2007. [doi:10.1115/ICNMM2007-30031](#).

## Acknowledgements

We thank Ian Ellerington for posing question in 2014 of calculating the velocity ratio correctly.

## Appendix A. Software used in this study

This document is written in L<sup>A</sup>T<sub>E</sub>X using the collaborative editor <https://www.overleaf.com>. The python code and input data is published on GitHub: <https://github.com/PhilipSargent/h2-in-pipes> under the MIT open source license[8].

## Appendix B. Compressibility

All calculations in this paper have used an equation of state and mixing rules appropriate to the pressure and temperature for each pure gas or blend studied. Individual corrections are small, but they multiply together to make a significant difference.

### Appendix B.1. Equation of state

To calculate the compression factor as a function of temperature and pressure, and for gases such as natural gas composed of several different compounds, one needs an equation of state. The low pressures and ambient temperatures of the distribution grid mean that several different equations of state are all sufficiently accurate.

Lozana *et al.* have recently reviewed[42] the relevant equations of state and there are a bewildering variety of suitable functions. In this paper we use the 1978 Peng-Robinson equation of state[24], with temperature dependent binary interaction parameters and no volume translation corrections.

Equations of state for gas mixtures are still an active research area and there is continual development of alpha functions, interaction parameters and mixing rules e.g. Pina-Martinez *et al.*[43]. For the exact calculation method used in this paper, see Appendix F.1 and the code[8].

## Appendix C. Dew point and partial pressure

Our calculations produce the partial pressure of water vapour in the flue gas, but we need the dew point. The two are related by standard tables of the saturation vapour pressure of water[18]: the pressure at which water vapour is in thermodynamic equilibrium with its condensed state.

There are several explicit formulae which model the vapour pressure of water as a function of temperature, but the dew point temperature is very sensitive to slight inaccuracies. For example, the commonly used Antoine equation would get the dew point incorrect by nearly 2°C.

The range of atmospheric pressure in the UK means that the dew point of the flue gas varies  $\pm 1.4^\circ\text{C}$ , which affects the maximum efficiency.

## Appendix D. Upgrading UK Boilers

In the most recent English housing survey[44], approximately one tenth ( $7/(59+7)$ ) of domestic boilers on piped-gas were non-condensing and nine-tenths condensing: "the proportion of dwellings with a standard boiler decreased from 9% in 2020 to 7% in 2021, while the proportion with a condensing-combination boiler has increased from 57% to 59% in the same period".

However there are no statistics on how many of the condensing boilers have correctly-adjusted  $50^\circ\text{C}$  return-flow settings with appropriate weather compensation. Anecdotally, the proportion is very small, very likely less than 5%. So a reasonable estimate would be that the return temperature is set to  $50^\circ\text{C}$  for 5% of the condensing boilers and to  $70^\circ\text{C}$  for 95% of the them. There is no condensing for the non-condensing boilers so their efficiency is simply the Lower Heating Value, i.e. a 'condensation' temperature of  $100^\circ\text{C}$ .

So when calculating an efficiency multiplier when converting from natural gas to hydrogen, we will assume

- That 4% of boilers are already perfectly adjusted, and the only change will be the multiplier of  $0.974\times$  from the change in fuel condensation behaviour
- That 86% of boilers will go from a condensing temperature of  $70^\circ\text{C}$  (87.44% with NG) to  $50^\circ\text{C}$  (93.69% with hydrogen), a multiplier of  $0.933\times$
- That 10% of boilers will change from an efficiency of 86.20% (non condensing) to a fully-condensing, properly adjusted reflow temperature of  $50^\circ\text{C}$  (93.69% with hydrogen), a multiplier of  $0.920\times$

The population weighted efficiency multiplier is thus  $0.933\times$ .

## Appendix E. Viscosities

The viscosities of pure components are calculated from experimental data as a least-squares fit to a power law dependence on absolute temperature. Ideal gases have a

power law relationship where the exponent is 0.5, the real gases here have exponents between 0.66 and 1.08. The viscosity of the gas mixture is a molecular fraction weighted average[45] of the viscosities of the components.

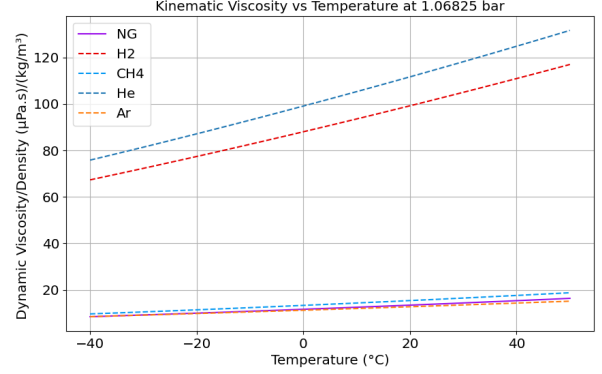


Figure E.5: Plot of kinematic viscosity: the ratio of dynamic viscosity and density, as a function of temperature

Figure E.5 shows the temperature dependence of the kinematic viscosities (the ratio of density to dynamic viscosity) of the natural gas blends. This shows why it is important to do these calculations at a well-chosen reference temperature rather than using textbook values which may have been measured at a variety of different temperatures.

In the UK the ground temperature of the gas in the buried LP network is likely to stay in the range 5 to  $15^\circ\text{C}$  all year.

### Appendix E.1. Laminar flow

If the gas velocity on a summer night is sufficiently slow that both the natural gas and the hydrogen fall within the laminar flow regime, then the pressure drop is linear in both velocity and viscosity. The viscosity ratio is 0.8209 at  $8^\circ\text{C}$  and the velocity ratio, which is unchanged, is 3.080. Thus, the pressure drop ratio is 2.528

The compressor power required to deliver it will be the velocity ratio times the pressure drop ratio, i.e.  $7.787\times$  greater.

Table E.6: Laminar flow – at  $8^\circ\text{C}$

	Ratios for H2/NG
velocity	$3.080\times$
pressure drop	$3.080\times$
power reqd.	$7.787\times$

### Appendix E.2. The Blasius parameter materials property

Note that the term  $\rho^{3/4} \cdot \mu^{1/4}$  in equation 13 is a materials' property which depends on temperature and pressure. We define this property as B, the Blasius parameter in equation E.1.

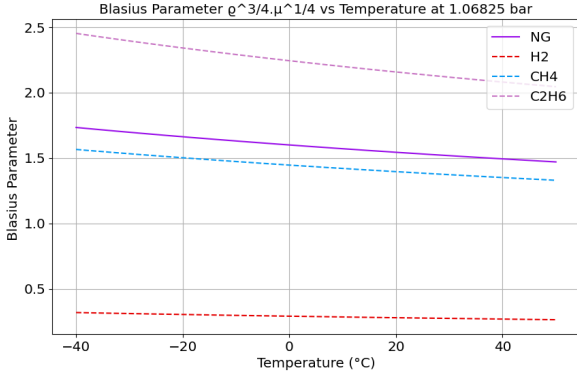


Figure E.6: Blasius Parameter  $\rho^{3/4} \cdot \mu^{1/4}$  ((kg/m)·(m·s)<sup>-4</sup>)

$$B = \rho^{3/4} \cdot \mu^{1/4} \quad (\text{E.1})$$

where  $\rho$  is the density and  $\mu$  is the dynamic viscosity.

Somewhat surprisingly, this materials' property has only a slight dependence on temperature as the dependencies of density and viscosity act in opposite directions.

Also surprisingly, all the gases in the study have very similar dependence such that the normalised Blasius parameter, where the value for each gas is divided by the value for natural gas, is very nearly independent of temperature, varying less than 1.2% between -40°C and +50°C.

This means that results calculated using the Blasius parameter, the relative pressure drop and the relative compression power requirement, are independent of temperature in the distribution grid.

### Appendix E.3. Wobbe number and reference temperatures

At 15°C the Fordoun gas has a density of 0.81507 kg/m<sup>3</sup>, an HHV of 39.8902 MJ/m<sup>3</sup>, and a Wobbe number<sup>15</sup> of 49.97451 MJ/m<sup>3</sup>.

In the UK 15°C is the temperature for assessing allowable<sup>16</sup> Wobbe limits[13, 47]. Wobbe values of fuel gases are sensitive to temperature via the effect of temperature on gas density and molar volume and the distinction between 15°C and the industry informal standard of 0°C is significant. However, despite ISO 13443, the 25°C reference heat of combustion always seems to be used in practice for Wobbe calculations.<sup>17</sup>

This paper does not use Wobbe numbers in any of the calculations.

## Appendix F. The Peng-Robinson calculations

### Appendix F.1. Calculating the properties of a gas mixture

The higher heat capacity and the mean molecular weight of the Fordoun natural gas are calculated from a mole fraction weighted sum of those properties of the component pure gases.

The compressibility and density of the natural gas are calculated for a given temperature and pressure using the Peng-Robinson equation of state:

1. The Peng-Robinson[43] parameters  $a$  (attraction) and  $b$  (repulsion) for each pure component at a given temperature are calculated from the critical temperature  $T_c$ , the critical pressure  $P_c$ , and the  $\omega$  coefficient (a measure of the molecule asphericity) of each pure gas.
2. the coefficient  $b$  of the mix is the weighted sum of the  $b$  values of the component gases, where the weights are the mole fractions.
3. The temperature dependent binary interaction parameter  $k$  is calculated using the Courtinho method[48] from the  $b$  value of each gas in a pair. For an 11 component gas there are 55 pairwise interactions.
4. The  $a$  values are calculated as the weighted sums of the geometric means of the pair-wise values of  $a$  between each pair of components. The weights are the mole fractions of each pair multiplied together, times the value  $(1-k)$
5. The effective  $T_c$ ,  $P_c$  and  $\omega$  of the natural gas, the pseudo-component, are calculated from the  $a$  and  $b$  values for the mix for the given temperature
6. the compressibility and thus the density of the natural gas is calculated using the effective  $T_c$ ,  $P_c$  and  $\omega$  values.

The precise algorithm is in the code on GitHub[8].

The published paper is likely to be limited to 12 pages.

<sup>15</sup>The Fordoun gas is thus centrally within the regulatory limits.

<sup>16</sup>The multiplicity of "standard reference conditions" of temperature, pressure and humidity (state of saturation) used in the measurement of natural-gas quality and quantity can cause much confusion', ISO 13443[46]

<sup>17</sup> ISO 13443 defines standard reference conditions of 15°C and 1.01325 bar for use with natural gases and natural gas substitutes. ISO 6976 was substantially revised in 2016 and data, especially Wobbe data, from papers published before then should not be re-used without being re-evaluated[47]



## Appendix G. Lower Heating Value (LHV) and process heat

Some users on the distribution network use gas for process heat; for an oven, furnace or kiln. Replacing natural gas with hydrogen for these users means that the velocity factor, the ratio of the gas velocity for hydrogen and natural gas, is the ratio of the gases' LHV in  $\text{kJ}/\text{m}^3$ .

There is no generally agreed way of defining LHV unless the exit temperature of the flue gas is specified. If the latent heat of the water is simply subtracted from the HHV, that is equivalent to saying that the flue gas exits at  $25^\circ\text{C}$  which would be quite wrong. For a bread oven it would be about  $190^\circ\text{C}$  whereas a pottery kiln could be up to  $1,400^\circ\text{C}$ .

## Appendix H. 16km visualisation

A way of visualising the network characteristics is to imagine a single 110 mm diameter pipe carrying the natural gas with 75 mbar pressure at one end and 20 mbar pressure at the other with a velocity of  $1.73 \text{ m/s}$ <sup>18</sup> and  $Re = 11,849$ . We use the Darcy-Weisbach equation (equation 9) and rearrange to get

$$Length = \left( \frac{2 \cdot \Delta P}{0.079} \right) \cdot \rho^{-3/4} \cdot \mu^{-1/4} \cdot v^{-5/4} \cdot D^{5/4} \quad (\text{H.1})$$

$$\begin{aligned} \Delta P &= (75 - 20)/1000 \text{ bar} \\ \rho^{-3/4} &= (0.84148)^{-3/4} \rho : (\text{kg}/\text{m}^3) \\ \mu^{-1/4} &= (10.37391 \cdot 10^{-6})^{-1/4} \mu : (\mu\text{Pa}\cdot\text{s}) \\ v^{-5/4} &= (1.7323)^{-5/4} v : (\text{m}/\text{s}) \end{aligned}$$

Solving this we find that this pipe would be about 16 km long .

If we imagine that this was representative of the UK gas demand in 2004, then in 2021 the reduced amount of gas (77.2%) would mean that the velocity would reduce in proportion and the pressure drop would reduce. So if the high pressure end was maintained at 75 mbar the pressure at the low pressure exit would rise to 40.03 mbar.

If we now replaced the gas with pure hydrogen delivering the same useful energy flowing at  $3.08\times$  the velocity then the pressure at the domestic end would be 29.7 mbar with a Reynolds' number of 4,868. So with hydrogen, even though it requires a higher pressure drop, this example network would still have 'headroom' of 9.7 mbar above the domestic exit limit of 20 mbar.

## Appendix I. UK Boilers in yet more detail

The gradient of the condensation curve of Fig.2 is shown in Fig. I.7. For a hydrogen boiler, the increase in efficiency per degree cooling peaks at  $0.009 \text{ \%}/\text{K}$  at the dew point.

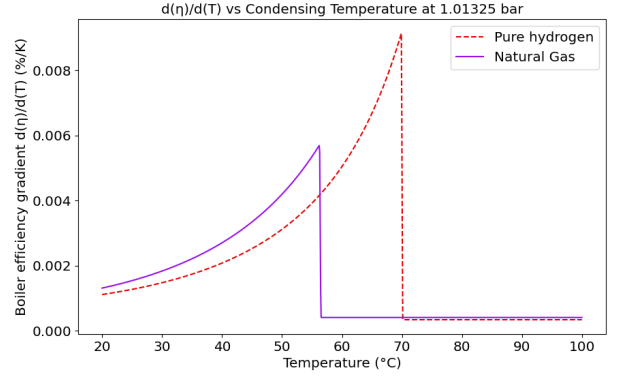


Figure I.7: How the efficiency of the boiler changes for each degree that the condensation temperature reduces.

### Appendix I.1. Published boiler efficiencies

Boiler efficiency[34] is measured either in a test rig at steady-state load, or estimated as a seasonal average as installed in a house with a typical daily heating cycle and weather pattern. Repeated on- and off-periods increase losses[15]. Boiler manufacturer published efficiency values may be legally-required in some jurisdictions to be a seasonally-adjusted average number.

### Appendix I.2. Hydrogen upgrade boiler controls

When considering a transformation to 100% hydrogen, every boiler will require replacement or systemic upgrade, and it would be reasonable to expect that as well as setting correct return temperatures, modern weather-compensating controls would be installed at the same time. This would have a dramatic effect on the energy demand of the UK housing stock and significantly reduce the quantity of hydrogen required over the year - though not on cold days during peak demand hours.

### Appendix I.3. Solubility of Carbon Dioxide

There is one extra effect which means that the Higher Heating Value for natural gas is a very slight underestimate of what is achievable.

The standard heat of combustion is derived assuming that the resultant gases are in their standard state at  $25^\circ\text{C}$  and one atmosphere. For  $\text{CO}_2$  this will not be true: in a condensing boiler some of the  $\text{CO}_2$  will preferentially dissolve in the condensing water and this is (overall) an exothermic reaction generating more heat.

The solubility of  $\text{CO}_2$  is about 0.004% mole fraction[49] at  $20^\circ\text{C}$  and at a partial-pressure of 0.09 bar (8.94% mol/mol in Table 3), and it is less soluble at higher temperatures, so the effect on the HHV is very small.

In a boiler burning pure hydrogen, there is no effect as there is no  $\text{CO}_2$ .

<sup>18</sup> This is the gas velocity when the domestic meter maximum of  $6 \text{ m}^3/\text{s}$  of gas is delivered to a single household through a 35 mm pipe.



## Appendix J. 20% Hydrogen in Natural Gas

UK standards state that boilers installed since 1996 must be capable[3] of combusting up to 23% hydrogen. However when burning 100% hydrogen, the internals of the boiler would need to be significantly changed because of flame velocity issues.

When considering hydrogen being introduced as a partial blend into the gas network, it is appropriate to assume that the population of boilers will require no systemic maintenance or upgrades if the percentage of hydrogen is 20% or less as this is the purpose of limiting the addition to 20%.

All efficiency calculations of properly adjusted condensing boilers assume that the heat exchanger is perfect, with all water condensed at the reflow temperature. In reality there will be an additional loss. When adding hydrogen, the velocity of the *flue* gas increases by an amount which is quite different from the increase in velocity of the *fuel* gas. This increased flue gas velocity is likely to degrade the efficiency of the the exchanger through these opposing effects:

1. Increased shear at the exchanger walls[34] increases heat transfer rate,
2. Decreased residence time of the flue gas in the heat exchanger

It is the second of these which is likely to be the more significant effect. So for a fixed exchanger geometry and return water flow, the flue gas exit temperature will be higher when burning some hydrogen.

Therefore while in principle we might attempt to estimate the change in efficiency of the entire boiler population, we cannot actually estimate the effect on the flue gas heat exchanger without experimental data.

Thus we should expect that a pure hydrogen boiler would need a redesigned, longer heat exchanger for the flue gas exit temperature to be the same as it would be for a natural gas boiler.

Therefore, although the maximum possible efficiency for a condensing boiler increases when the fuel is switched to hydrogen, the actual operating efficiency will be very dependent on individual heat exchanger parameters[20, 22].

### Appendix J.1. Boiler overcapacity

There is likely to be significant heating capacity headroom with existing domestic boilers, which are almost invariably oversized[32]<sup>19</sup> as shown in Fig J.8.

However this tells us little about whether the Service Line low pressure distribution network is oversized.

<sup>19</sup>Where domestic heating is inadequate, this is almost invariably due to inappropriate ventilation, piping, radiators or controls.

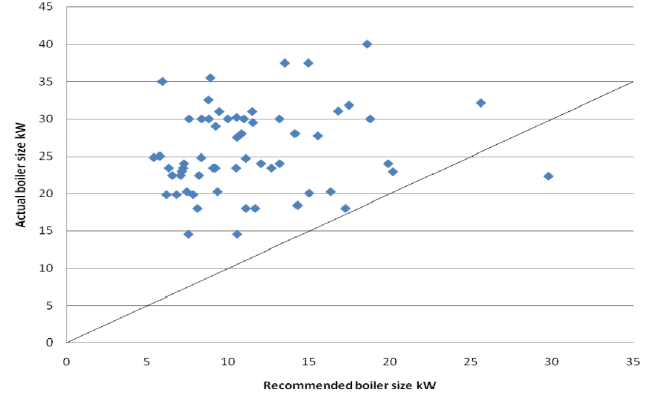


Figure J.8: Example data from the Energy Saving Trust[22] illustrating that nearly all UK boilers are oversized.

## Appendix K. Annual power requirement

### Appendix K.1. annual average

There is no good public data on the energy used to compress natural gas across the UK transmission network. The distribution network is entirely passive: there are no compressors, only pressure reduction systems. So the compression energy calculated here for the distribution system will actually be supplied by compressors on the transmission system.

UK gas demand has vast daily and seasonal variations. There is perhaps only 10% of the demand at night, during the summer, and there is a substantial dip in the middle of the day even in winter.

While the peak gas demand is well documented, much of the gas, perhaps half, will be delivered when the gas velocity is much lower than at peak. However, the instantaneous relationships between the flow of natural gas and the flow of hydrogen still holds (so long as all flows are within the Reynolds' number range of the Blasius flow) so the annual energy cost of delivering hydrogen over delivering natural gas will be  $3.994\times$ .

### Appendix K.2. Pressures of UK gas pipelines

This paper only considers the low pressure and service pipes.

Table K.7: Pressures of UK gas pipelines[1]

		(bar)
Transmission	Transmission	70–94
Distribution	High Pressure	7.0–30.0
	Intermediate Pressure	2.0–7.0
	Medium pressure	0.075–2.0
	Low pressure	< 0.075
Service	Building connections	> 0.019, < 0.075

### Appendix K.3. Leaks

The generally expected result of changing from natural gas to hydrogen is an increase in the volume of gas leaked, because of the lower viscosity and slightly higher pressure with hydrogen, but a lower loss of combustive energy.

Leaks are through small holes or planar cracks. Given this geometry, leaks (especially of hydrogen) will have very low Reynolds' numbers and will be in the laminar flow regime if they are long and deep, otherwise they will be in the orifice-flow regime .

### Appendix L. Darcy-Weisbach Reynolds-Blasius material parameter

See Figure L.9 to see that the Darcy-Weisbach Reynolds-Blasius material parameter 'B' (when normalised by the values for natural gas) varies by less than 1.2% over the temperature range.

However, when considering pressures of 4 and 7 bar (5 and 8 bar absolute), the assumption of nearly-ideal behaviour does not hold. The properties of the gas are not nearly linear, so one can not assume that the behaviour along a pipe can be treated as a simple average of the behaviour at each end.

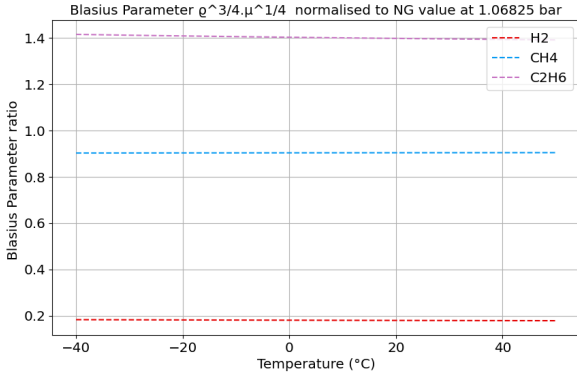


Figure L.9: Ratio of Darcy-Weisbach-Reynolds-Blasius material parameter to that of natural gas NG

Blasius Parameter  $\rho^{3/4} \mu^{1/4}$  normalised by the value for natural gas (Table 1) between -40.0°C and 50.0°C

### Appendix M. Flow at the turbulent transition

#### Appendix M.1. Hydrogen and Natural Gas comparative behaviour

If we look at how the friction factor changes when natural gas is replaced by hydrogen we get the family of curves in Fig.M.11.

When the velocity increases by a factor of 3.076 the Reynolds number decreases by a factor of 0.4103, at the pressure and temperature of the distribution service pipe.

When the flow is so low that both gases are in the laminar regime then the ratio of friction factor is a steady

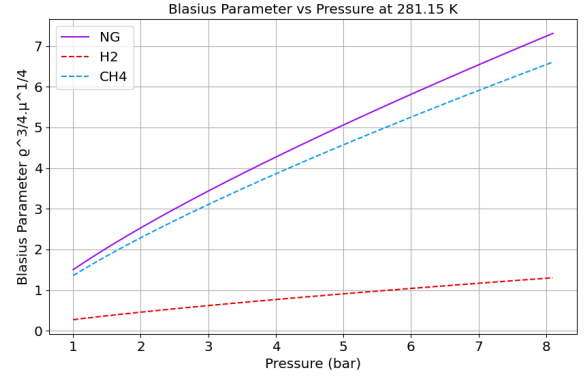


Figure L.10: Darcy-Weisbach-Reynolds-Blasius material parameter depends on pressure

Table L.8: Normalised 'B' Materials parameter gas/NG (-40.0°C to 50.0°C) showing temperature independence[8]

1.06825 bar			
H2	0.1813	± 0.0021	± 1.18%
CH4	0.9038	± 0.0007	± 0.08%
C2H6	1.4032	± 0.0119	± 0.85%
5.01325 bar			
H2	0.1794	± 0.0013	± 0.71%
CH4	0.9035	± 0.0009	± 0.10%
C2H6	1.4427	± 0.0300	± 2.08%
8.01325 bar			
H2	0.1779	± 0.0006	± 0.35%
CH4	0.9032	± 0.0010	± 0.12%
C2H6	1.4801	± 0.0499	± 3.37%

142% higher for hydrogen than for natural gas. At large Reynolds' number, the increase in friction factor is zero because in that regime the flow is not sensitive to Reynolds' number at all. This is the case for smooth pipe above  $Re = 2.10^6$

We find the ratio of the pressure drops for hydrogen and natural gas by taking the ratio of the two cases using equation 9, copied here as equation M.1.

$$\Delta p = f \left( \frac{L}{D} \right) \frac{1}{2} \rho v^2 \quad (M.1)$$

where  $L$  is the length of the pipe,  $D$  the diameter of the pipe,  $v$  is the mean velocity of the gas,  $\rho$  the density, and  $f$  the Darcy friction factor

$$\left( \frac{\Delta P_{H_2}}{\Delta P_{NG}} \right) = \left( \frac{f_{H_2}}{f_{NG}} \right) \left( \frac{\rho_{H_2}}{\rho_{NG}} \right) \left( \frac{v_{H_2}}{v_{NG}} \right)^2 \quad (M.2)$$

The terms in the ratios of  $\rho$  and  $v$  do not change as Reynolds' number changes, so the required pressure drop to produce the same energy delivery as for natural gas is a curve of the same form.

$$\left( \frac{\Delta P_{H_2}}{\Delta P_{NG}} \right) = \left( \frac{f_{H_2}}{f_{NG}} \right) \cdot 1.03512 \quad (M.3)$$

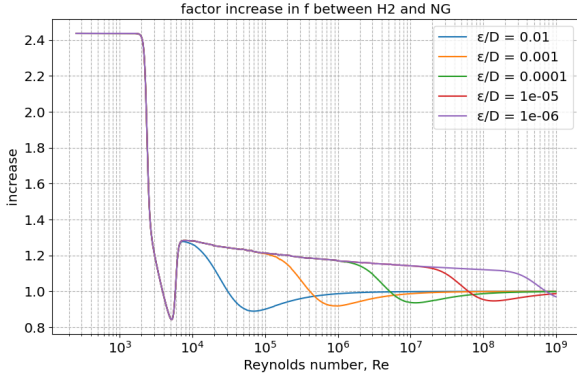


Figure M.11: Factor increase in Friction factor  $f$  when natural gas is replaced with hydrogen with a velocity ratio of 3.076 .

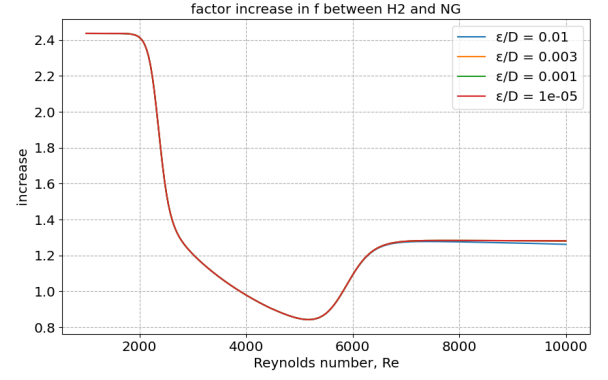


Figure M.13: Friction factor % increase when natural gas is replaced with hydrogen with a velocity ratio of 3.076 .

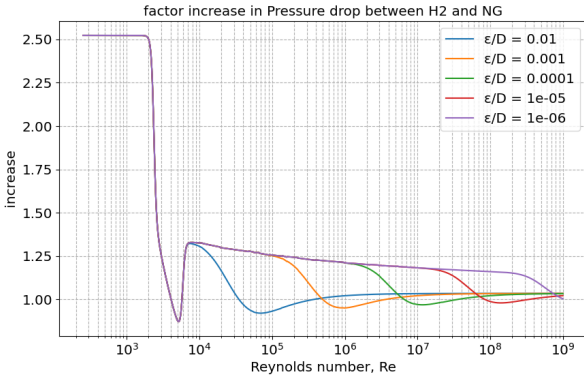


Figure M.12:  $\frac{\Delta P_{H_2}}{\Delta P_{NG}}$  % increase when natural gas is replaced with hydrogen with a velocity ratio of 3.076 and a density ratio of 0.1094 .

On reflection, one might wonder why the curve in Fig.M.12 has only one minimum, whereas each of the natural gas and hydrogen friction factor curves have their own minima. The resolution of this can be seen in Fig.M.13 where the double minima contributions can be seen in the shape of the single minimum.

#### Appendix M.2. Gioia and Chakraborty

Equation M.2 is generically true for all flow regimes where the Darcy-Weisbach relation holds. So it is not valid for higher pressure gases where the behaviour along the pipe is not linear because of pressure effects.

Equation M.4 Relates the friction factor ( $f$ ) to the Reynolds number ( $Re$ ) and the roughness parameter ( $r$ )[50]. (Note that this is the Fanning friction factor, equal to four times the Darcy-Weisbach friction factor). It is shown in Fig.M.14.

$$f = \frac{0.8}{(Re/A)^{\frac{1}{3}}} \left( 1 + \frac{12}{(Re/B)^2} \right)^{-\frac{1}{2}} \quad (M.4)$$

where the coefficients A and B are defined by M.5 in

terms of the roughness ratio  $r = \epsilon/D$ :

$$\begin{aligned} A &= 30 + 8.8r + 7.1r^2 + 2.4r^3 \\ B &= 550 + 33r^2 \end{aligned} \quad (M.5)$$

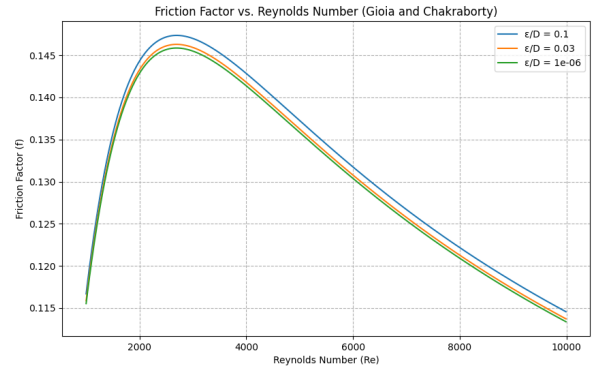


Figure M.14: Friction factor for all pipe roughnesses at the turbulent transition.

However Brackbill has shown that the critical Reynolds' number is roughness dependent (Figure 9 in [51]) and since 2018 it is now known that this is due to the time-average of laminar, slug and flash flow[30].

The Colebrook equation M.6 does not represent the Nikuradse 'hump' and 'belly' which recent research at Princeton and Okinawa shows is real.

$$\frac{1}{\sqrt{f}} = -2.0 \log_{10} \left( \frac{(\epsilon/D)}{3.71} + \frac{2.51}{Re\sqrt{f}} \right) \quad (M.6)$$

The Goldenfeld equation M.7 illustrates the form that any physically reasonable model should conform to[31].

$$f = Re^{1/4} \cdot g \left( (Re^{3/4}, \epsilon/D) \right) \quad (M.7)$$

It should be observed that none of the semi-empirical curve fits of Colebrook, Afzal, Swamee etc. conform.

“The Nikuradze data show four features: a hump, the Blasius regime, a shallow minimum, and the Strickler regime. The scaling argument presented here implies that the Blasius and Strickler regimes are both manifestations of inertial range scaling coupled with wall friction, and, indeed, Gioia and Chakraborty[50] find from momentum flux considerations that this is sufficient to reproduce the Blasius and Strickler regimes.”[31]

## Appendix N. Modelling Background

High-level economic models of hydrogen deployment use quite different, less detailed calculations for how hydrogen flows in an existing network than do detailed engineering designs.

These broad-brush models can unwittingly promote inaccurate intuitions which are not mere matters of detail. While it is true that pure hydrogen requires a volumetric flow rate nearly  $3\times$  that of natural gas to provide the same combustion power, it is not true that this requires pipelines  $3\times$  the size, or running an existing pipeline at  $3\times$  the pressure.

A techno-economic model needs simple formulae to describe technology choices. Unfortunately the voluminous technical literature on the delivery of hydrogen through pipes does not always present the results in a form that can be used, or even understood, by techno-economic modellers.

### *Appendix N.1. Policy making*

Techno-economic models need to evaluate required equipment capability at peak demand as this determines the capital expenditure. They also need to calculate the mean throughput over each year as this determines the running costs, e.g. the annual energy requirement for pumping hydrogen. But rather than central values for each of these, a policy-relevant model would produce upper and lower bounds. This means that upper and lower bounds on the friction values of hydrogen flows are useful, even if (as is the case) the actual turbulent behaviour is uncertain.